arXiv:0708.0280v1 [cond-mat.str-el] 2 Aug 2007

Searching for Stable Na-ordered Phases in Single Crystal Samples of γ-Na_xCoO_2

G. J. Shu[1], Andrea Prodi[2], S. Y. Chu[3], Y. S. Lee[2], H. S. Sheu[4] and F. C. Chou[1,4,†]
[1] *Center for Condensed Matter Sciences, National Taiwan University, Taipei 10617, Taiwan,*
[2] *Department of Physics, Massachusetts Institute of Technology, Cambridge, MA 02139*
[3] *Center for Materials Science and Engineering, Massachusetts Institute of Technology, Cambridge, MA 02139*
[4] *National Synchrotron Radiation Research Center, HsinChu 30076, Taiwan*

(Dated: February 8, 2022)

We report on the preparation and characterization of single crystal γ phase Na_xCoO_2 with $0.25 \leq x \leq 0.84$ using a non-aqueous electrochemical chronoamperemetry technique. By carefully mapping the overpotential versus x (for $x < 0.84$), we find six distinct stable phases with Na levels corresponding to $x \sim 0.75$, 0.71, 0.50, 0.43, 0.33 and 0.25. The composition with $x \simeq 0.55$ appears to have a critical Na concentration which separates samples with different magnetic behavior as well as different Na ion diffusion mechanisms. Chemical analysis of an aged crystal reveals different Na ion diffusion mechanisms above and below $x_c \sim 0.53$, where the diffusion process above x_c has a diffusion coefficient about five times larger than that below x_c. The series of crystals were studied with X-ray diffraction, susceptibility, and transport measurements. The crystal with $x = 0.5$ shows a weak ferromagnetic transition below $T = 27$ K in addition to the usual transitions at $T = 51$ K and 88 K. The resistivity of the Curie-Weiss metallic $Na_{0.71}CoO_2$ composition has a very low residual resistivity, which attests to the high homogeneity of the crystals prepared by this improved electrochemical method. Our results on the various stable crystal compositions point to the importance of Na ion ordering across the phase diagram.

PACS numbers: 61.10.Nz, 61.50.Nw, 66.30.-h, 75.20.Hr, 75.30.Cr, 71.27.+a

I. INTRODUCTION

The lamellar cobaltates Na_xCoO_2 have attracted much attention since the discovery of superconductivity in the hydrated composition $Na_{0.3}CoO_2{\cdot}1.4H_2O$.[1] The complete phase diagram of Na_xCoO_2 shows a variety of rich phenomena, such as A-type antiferromagnetic (AF) ordering for $x \sim 0.75$, large thermopower enhancement for $x = 0.85$, and AF ordering with a metal-to-insulator transition for $x = 0.5$.[2,3,4,5,6] Na_xCoO_2 is composed of alternating layers of Na and CoO_2, where the Na ions are surrounded by six oxygens which form a prismatic cage in the γ phase.[7] Sodium de-intercalation in powder samples has been effectively performed via chemical extraction, such as a topochemical process using a Br_2/acetonitrile solution.[1] We have demonstrated previously an electrochemical method as an alternative route to produce homogeneous compounds using a controlled overpotential (above the open circuit potential).[8] Using an aqueous $NaOH/H_2O$ solution as the electrolyte, high quality single crystals were obtained, and measurements of their conducting, superconducting and magnetic properties have been reported.[9,10] However, detailed studies of the voltage versus Na concentration diagram for $x < 1/2$ have been hindered due to difficulties related to an oxygen evolution side-reaction in the aqueous solution.[8]

Na ordering - in particular its impact on the geometry of the Fermi surface - is a key issue that requires further study in order to better understand the transport and magnetic properties.[4,9,11,12,13] Local density approximation (LDA) calculations indicate that a band with a_{1g} character should create a large hexagonal Fermi surface centered around the Γ point.[11] The existence of such a large Fermi surface has been verified from angle-resolved photo-emission(ARPES).[14,15] However, subtle effects due to possible superstructure formation and/or strong electron correlation remain elusive, such as the missing small hole pockets predicted by LDA calculation. Bobroff *et al.* proposed a nesting scenario based on an orthorhombic reduced Brillouin zone caused by Na ordering to interpret the antiferromagnetic and metal-to-insulator transitions found in $Na_{0.5}CoO_2$.[4] A reconstructed Fermi surface may also explain the small hole pocket found in $Na_{0.5}CoO_2$ and $Na_{0.3}CoO_2$ by Shubnikov-de Haas oscillation measurements.[9,16] Several superstructures have been observed and modeled from electron diffraction studies of Na_xCoO_2 with x between 0.15 and 0.75.[17] Calculations based on electrostatic interaction between Na ions alone have been used to propose several types of Na ordering patterns.[18] Other calculations point to the importance of the coupling between Na-vacancy ordering and Co^{3+}/Co^{4+} charge ordering, indicating that Na^+–Na^+ repulsion and the Na(1)–Na(2) site energy dif-

ference alone is not enough to describe the observed superlattices.[19] A recent neutron diffraction study and associated numerical simulations have elucidated aspects of the Na ordering in single crystals of Na_xCoO2 with x $\sim$ 0.75 - 0.92.[20]

Much still remains to be understood regarding the possible Na ordering patterns across the phase diagram. Currently, Na ordering has been studied mostly in samples with $x = 1/2$ and $x \simeq 3/4$. However, reproducibly preparing precise stoichiometries of these phases is not straightforward. Many early studies of samples with $x = 0.7 - 0.9$ did not pay much attention to the exact ordering of Na ions and often assumed substantial defect formation due to Na loss at high temperatures.[21] Although $Na_{0.5}CoO_2$ shows the highest ordering and phase stability among the Na_xCoO_2 series, phase inhomogeneity and phase separation have been discussed based on electron microscopy studies of $Na_{0.5}CoO_2$.[17,22] A reliable procedure for controlling the Na content and the rate of de-intercalation of single crystal samples of Na_xCoO_2 is highly desirable, especially in light of the possibility of producing Na ordered phases.

We find that an electrochemical method which carefully controls the overpotential at the sample surface is a particularly reliable route that can approach the real equilibrium state and, moreover, is suitable for single crystal samples. The topochemical method is an effective method to produce powder samples as reported previously.[23] However, the Na level in powders is more susceptible to Na loss due to the much shorter diffusion path and significantly larger surface-to-bulk ratio. In fact, we find that over time, Na diffusion under normal storage conditions can affect surface layer stoichiometry as deep as 50 μm as we discuss below. Here, we have used electrochemistry in a non-aqueous solution to carefully prepare a series of homogeneous single crystals. Characterization of these samples reveals that six distinctively stable phases fall in the stoichiometry of $x \sim 0.75$, 0.71, 0.50, 0.43, 0.33 and 0.25. Most phases are clearly near simple commensurate filling fractions, while 0.71 and 0.43 require further modeling and simulation. Magnetic susceptibility and transport measurements have been performed on these samples and the results are discussed.

II. EXPERIMENTAL

All single crystals in this study were cleaved from a crystal grown using the floating-zone method as described previously.[10,24] In order to minimize any possible Na content differences between the surface and bulk, we performed all electrochemical experiments using thin crystals with thicknesses as small as 100 μm. The electrochemical cell was assembled using crystal sample as working electrode, Pt as counter electrode, and Ag/AgCl with sieved liquid junction as reference electrode. In contrast to our previous work, a non-aqueous electrolyte was used: 1N $NaClO_4$ in propylene carbonate. Single crystals of $Na_{0.84}CoO_2$ with size near 2×2×0.1 mm^3 were sandwiched into a spring-loaded cell to make the working electrode. A DC voltage V_{app} was applied between the working and reference electrodes at each applied voltage step, spanning the range from -0.25 V to 2.5 V relative to the Ag/AgCl reference. Equilibration is achieved by waiting until the induced anodic current reaches saturation and maintained for at least 12 hours. For chemical analysis of the stoichiometry, electron probe microanalysis (EPMA) was performed on freshly cleaved inner surfaces. To avoid electron-beam damage, EPMA data were collected using a low beam energy of 15 keV for 1 min duration on each fresh spot. Structural and bulk magnetic data were obtained from X-ray diffraction and SQUID magnetometry measurements, respectively. For the X-ray diffraction, single crystal samples were oriented, and the (00L) reflections at high angles were used to determine the c-axis. In-plane resistivity data of our various samples were obtained by performing four terminal DC measurements on single crystal samples. The crystals were cut to $1mm \times 0.5mm \times 0.1mm$ average size. The leads were attached with DuPont 4922N silver paint on a cleaved ab surface and dried in air, yielding contact resistances between $5 - 20\Omega$.

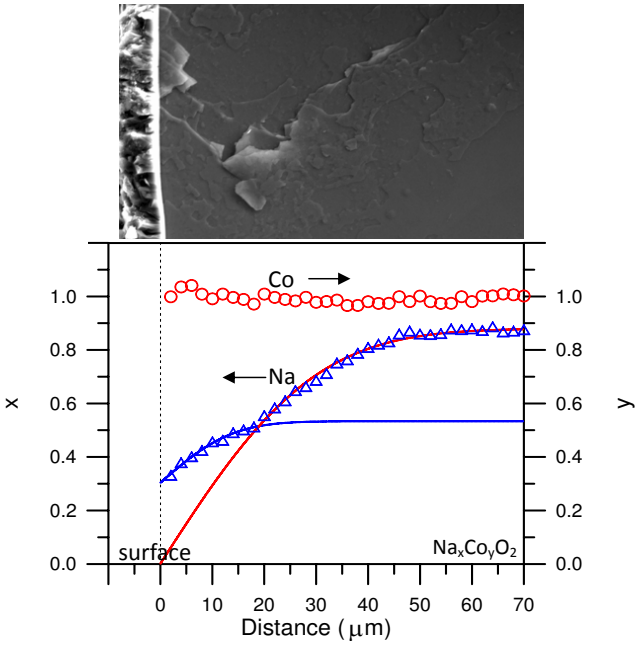

FIG. 1: (Color online)(a) SEM image of an "aged" ($\sim$ 2.5 years) crystal of $Na_{0.88}CoO_2$ cleaved with the c-axis perpendicular to the plane The left edge corresponds to the surface of the as-grown rod. (b) EPMA analyzed chemical concentration x as a function of distance from the crystal surface towards the interior of the rod. Solid lines are fits with a 1D diffusion model as described in the text.

III. RESULTS AND ANALYSIS

1. Sodium ion self diffusion

When the as-grown single crystal of Na_xCoO_2 with $x > 0.7$ is not stored properly within a moisture-free environment, a white precipitate builds up on the surface. We believe the surface Na ions readily react with the water in the air to form white NaOH precipitate. The vacated sites would induce further Na ion self diffusion. In order to better understand the diffusion mechanism of Na ions, we have examined the Na distribution profile of an "aged" single crystal of $Na_{0.88}CoO_2$ that has been stored in ambient environment of average humidity of 55% for about two and a half years. The original single crystal was prepared using floating-zone method as reported previously.[10] The "aged" crystal rod had a layer of white precipitate built up on the surface of the boule. We performed EPMA to examine the Na/Co ion distribution on a cleaved surface (*ab*-plane) which extends radially from the core area to the edge of the rod as shown in Fig. 1(b). An SEM photograph is shown in Fig. 1(a), where the crystal surface is defined as the zero position. We find that the Na concentration rapidly drops from $x \simeq 0.88$ in the interior of the rod to $x \simeq 0.3$ at the surface layer within a depth of $\sim$50 μm. The white layer outside the crystal consists of a rich concentration of Na (Na/Co > 1.67) and has been confirmed with X-ray diffraction to be NaOH. The Na^+ ions, with ionic radius $\sim$ 1.02 Å, may diffuse through the rectangular pores of threshold radius $\sim$ 0.91 Å formed by the oxygen ions of the NaO_6 prismatic cage.[25] Since Na^+ ions diffuse along the *ab*-plane toward the surface boundary through a vacancy hopping mechanism, the observed Na distribution shown in Fig. 1 would follow Fick's second law. The diffusion topography $c(r,t)$ and the diffusion coefficient $D_\circ$ can be described by the diffusion equation $\frac{\partial c(r,t)}{\partial t} = D_\circ \frac{\partial^2 c(r,t)}{\partial r^2}$ in one dimension. Although it is tempting to fit the whole data set with a single diffusion coefficient, we note the $c(r,t)$ profile has a pronounced crossover near $x \sim 0.5$. The best fit is obtained under the assumption of two different diffusion coefficients above and below the crossover point, as indicated by the solid lines in Fig. 1. Leaving the boundary conditions of $c(r,t)$ at the crossover point and the surface edge as free fit parameters, the best fit values of $D_\circ$ are $\sim$ 3.49 and 0.76×10^{-14} cm^2/s for diffusion above and below the crossover point, respectively. We note that this is close to the lower limit of D_{Li} for Li_xCoO_2 reported in the literature.[26] The diffusion coefficients extrapolated from single crystals are less susceptible to errors due to geometric factors and electrolyte permeation, compared to powder samples.

Interestingly, the observed crossover point is $x_c \sim 0.53$, which is just above half filling. The end point at the surface boundary is near $x \sim 0.30$, right below 1/3 filling. The fit value of $D_\circ$ for $x > 0.53$ is nearly five times of that from below. This indicates two distinctly different types of diffusion species dominated above and below half filling, which are most likely to be Na vacancy and Na^+ ion, respectively. For Na_xCoO_2 with x > 0.5, vacancy ordering is expected as demonstrated by the di-vacancy or tri-vacancy ordering patterns proposed by Roger *et al.*[20] In the multi-vacancy model, energy is gained through Na(2) vacancy cluster formation plus promotion of additional sodium ions from the preferred Na(2) site to Na(1) site. The larger diffusion coefficient for vacancy-dominated diffusion is also reflected in the lower overpotential required in electrochemical de-intercalation process, as will be discussed below. The concentration near the surface boundary is very close to $x = 1/3$, which is exactly the Na concentration that becomes superconducting after fully hydrated.[27] The energy gap between $x = 1/3$ and $x = 1/4$ appears to be large enough to prevent additional Na loss from the surface. The crossover point near $x_c = 0.53$ also separates the two main classes of magnetic behavior within Na_xCoO_2, i.e. the Curie-Weiss metal above and Pauli paramagnetic metal below.[3] The observed different diffusion mechanisms and thus different Na (vacancy) ordering patterns have shown profound influence on the magnetic and conducting properties of Na_xCoO_2.

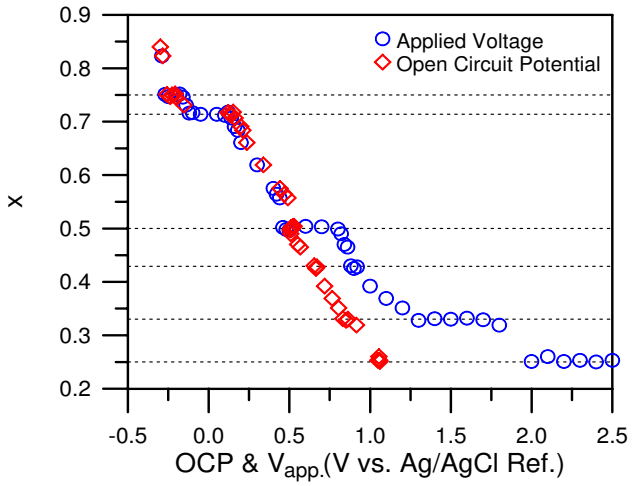

FIG. 2: (Color online) Na concentration x versus applied voltage V_{app} and open circuit potential (OCP), where x is obtained from EPMA analysis.

2. Electrochemical de-intercalation

The electrochemical de-intercalation method relies on the sharp concentration gradient at the sample/electrolyte interface. Na ions diffuse to the surface layer due to the non-zero overpotential until a new equilibrated surface chemical potential is reached. A plot of of the Na concentration (determined using EPMA) versus the applied electrochemical voltage (V_{app}) is shown in Fig. 2 for our single crystal samples. As the applied voltage increases, the Na content decreases similar to previously reported results on powder samples.[7,8] The stability of the resulting phases is evidenced by the wide plateau near regions of $dV_{app}/dx = 0$ at x near 0.71, 0.5, 0.33 and 0.25.

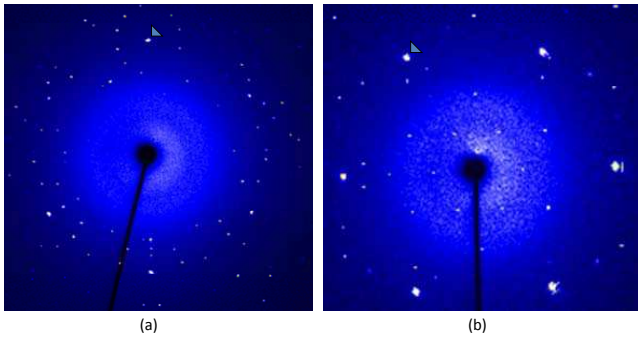

FIG. 3: (Color online) Representative Laue photographs for (a) the starting crystal with $x = 0.84$ and (b) a de-intercalated sample with the lowest Na content $x = 0.25$. The six brightest spots have been identified to be {100} with $d = 2.83$Å indicated by the small triangle. For $x = 0.84$, there are 12 spots surrounding {100} in a ring-like pattern. For $x = 0.25$, orthorhombic superlattice peaks can be identified in addition to {100}.

Crystals prepared with applied voltages between 0.5 and 0.8 V show nearly constant Na content of $x = 0.5$. In addition, higher voltages near 1.3 – 1.6 V and 2.0 – 2.5 V produce samples with stable phases of x close to 0.33 and 0.25 respectively, which had been difficult to produce due to the high current side reactions in previous studies.[8] We also measured the open circuit potential (OCP) after each equilibrium phase is reached as shown in Fig. 2. The OCP is slightly higher than V_{app} for x > 0.5, but is significantly lower than V_{app} for $x < 0.5$ due to the side reaction. Since the OCP primarily reflects the surface energy, the trend of OCP $> V_{app}$ for $x > 0.5$ suggests the bulk is equilibrating with a V_{app} that is lower than the surface energy. The results shown in Fig. 2 provide us with new insights into the formation of phases below $x = 0.5$ using V_{app} instead of OCP. The plateaus in the $V_{app} - x$ plot indicate phase coexistence regions with $dx/dV_{app} = 0$ around ~ 0.5 ,1.3 and 2.0 V. The corresponding stables phases are near $x = 0.50$, 0.33 and 0.25, which are near the simple fractional fillings of 1/2, 1/3, and 1/4. Single crystal quality is demonstrated by transmission Laue photography as shown in Fig. 3 using synchrotron X-rays ($\lambda = 0.4959$ Å), where $x = 0.84$ is the original as-grown crystal and $x = 0.25$ is the most de-intercalated sample. A Na superstructure indicated by 12 peaks forming a ring surrounding (100) is observed, just like that reported in Ref.[20]. An orthorhombic superstructure is found in $x = 0.25$, which is different from that observed in $x = 0.5$ with electron diffraction.[17]. Details of the superstructure analysis will be presented separately.[28]

In addition to the expected phases such as $x = 1/2$, 1/3 and 1/4, stable phases of $x = 0.43$, 0.71 and 0.75 are also clearly visible in Fig. 2. Although most early reports suggest that $x = 2/3$ is a preferred equilibrated phase, it failed to show up in the V_{app} versus x data. This result is in agreement with the prediction from Density Functional Theory (DFT) calculation, which suggests $x = 2/3$ is not a ground state due to the lack of a commensurate Na ordering pattern.[18] Our data indicate that $x = 0.71$ is the most stable phase among 0.75, 0.71 and 0.67, as reflected on the significantly wider applied voltage range of the $dx/dV_{app} = 0$ plateau. The stable phase of $x = 0.71$ can be prepared with V_{app} between -0.1 – 0.1V, while $x = 0.75$ is barely defined by a plateau of width less than 60 mV. The $x = 0.75$ phase has been shown to be at the lower boundary of the range ($0.75 \leq x \leq 0.85$) for compositions that possess A-type AF ordering at low temperature.[29,30] In addition, $x = 0.75$ falls at the exact boundary that minor x fluctuations would separate Na(2) to occupy either high symmetry 2c (2/3, 1/3, 1/4) or low symmetry 6h (2x, x, 1/4) sites within the space group $P6_3/mmc$.[31] Such behavior indicates that $x = 0.75$ is likely to be a metastable transient phase rather than a truly equilibrated ground state. The $x = 0.71$ phase is very close to a simple fractional filling of 5/7 that has been predicted to be a ground state from Density Function Theory (DFT) model calculation;[18] however, there are many other choices for a simple fraction that are near 0.71. Roger *et al.* have proposed an ordering of multivacancy clusters within the Na layer for $x > 0.7$, i.e., Na ions shift from the preferred Na(2) site to the unfavorable Na(1) site that is directly on top of the Co ions to further reduce stabilization energy.[20]

Another equilibrated phase below half filling is $x = 0.43$. Although the $dx/dV_{app} = 0$ plateau for $x = 0.43$ is less pronounced than that for $x = 0.75$, the narrow plateau sits between two distinctly different slopes as shown in Fig. 2. Considering the dominant diffusion species for x > 0.5 are vacancy clusters, the diffusion species for $x = 0.43$ would be Na ions. The fact that 0.43 being close to a simple fractional filling of 3/7 suggests that Na ions partially fill a superlattice consisting of 7 Na ions per unit supercell. Indeed Na trimer ordering of simple hexagonal unit $\mathbf{a}' = \sqrt{7}\mathbf{a}$ has recently been observed on the surface of an in-situ cleaved $Na_{0.84}CoO_2$ crystal using scanning tunneling microscopy, where half of the Na ions ($x \sim \frac{0.84}{2}$) are supposed to occupy each cleaved surface pair equally.[32] Whether such 3/7 superlattice ordering exists within the bulk requires further Laue transmission diffraction analysis.

3. *Phase homogeneity*

One of the major concerns in the experimental study of Na_xCoO_2 compounds is the question of phase homogeneity. When Na ions are de-intercalated through topochemical or electrochemical routes, the remaining Na ions should rearrange to find the ground state for each Na layer while maintaining the original CoO_6 stacking. The c-lattice parameters for our series of crystals were determined with X-ray diffraction and are summarized in Fig. 4. Since Na_xCoO_2 samples have highly oriented at (00L) planes even after the crystal is pulverized, X-ray diffraction has been performed on aligned crystals

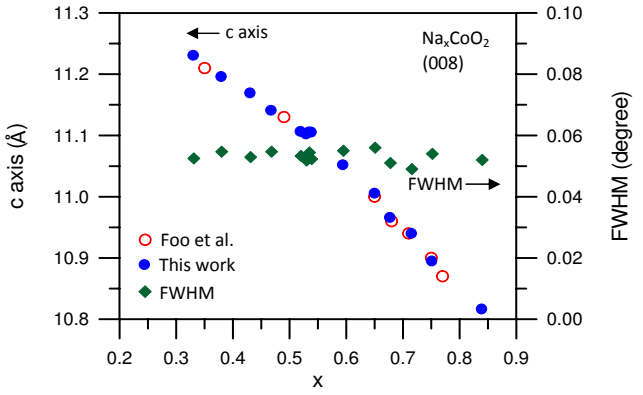

FIG. 4: (Color online) The c-lattice parameter of Na_xCoO_2 plotted against x. Crystal homogeneity is confirmed by the FWHM in 2θ of the (008) Bragg peak. The instrumental resolution is 0.05 degrees.

measuring the (00L) Bragg peaks. The c-axis is known to strongly depend on Na content as reported by several other groups.[3,33,34] Our c-axis lattice size is extracted from the (008) peak angle, and our results are consistent with those reported previously.[3] We notice the c-lattice parameter depends almost linearly on x with a weak deflection near $x \sim 0.55$. This behavior may suggest two regimes which follow the empirical Vegard's rule for substitutional impurities. The c-axis expansion as a function of lower x has also been reflected on the softening A_{1g} mode along the c-direction.[35] As shown in the inset of Fig. 4, phase homogeneity is evidenced by a consistently narrow full width at half-maximum (FWHM) for 2θ of the (008) peak. This width is comparable to our instrumental resolution limit, which is determined using a Si standard to be 0.05 degrees. The possibility of mixed-phase crystals is ruled out within our X-ray resolution limit for nearly all of the samples prepared by our method, except for samples prepared using V_{app} between 0.82 – 0.88 V as shown in Fig. 5. Two-phase behavior is observed within the narrow voltage range between 0.82 – 0.86 V, which corresponds to Na levels slightly below $x = 0.5$. The sample evolves from single phase of $x = 0.5$ to a single phase of $x = 0.43$ through mixed-phase intermediate states. In contrast, there is no two-phase signature observed between single phase $x = 0.55$ and $x = 0.5$. No other samples exhibited two-phase signatures regardless of whether V_{app} falls in the $dx/dV_{app} = 0$ plateau range. This suggests that phases of solid-solution without specific Na ordering do exist, at least in the time frame of days during preparation and characterization. Since the FWHM of (00L) peaks provide us only with coherence information along the c-axis, it is possible that in-plane ordering may yield potential microscopic phase separated domains as commonly found in this series.[17,22]

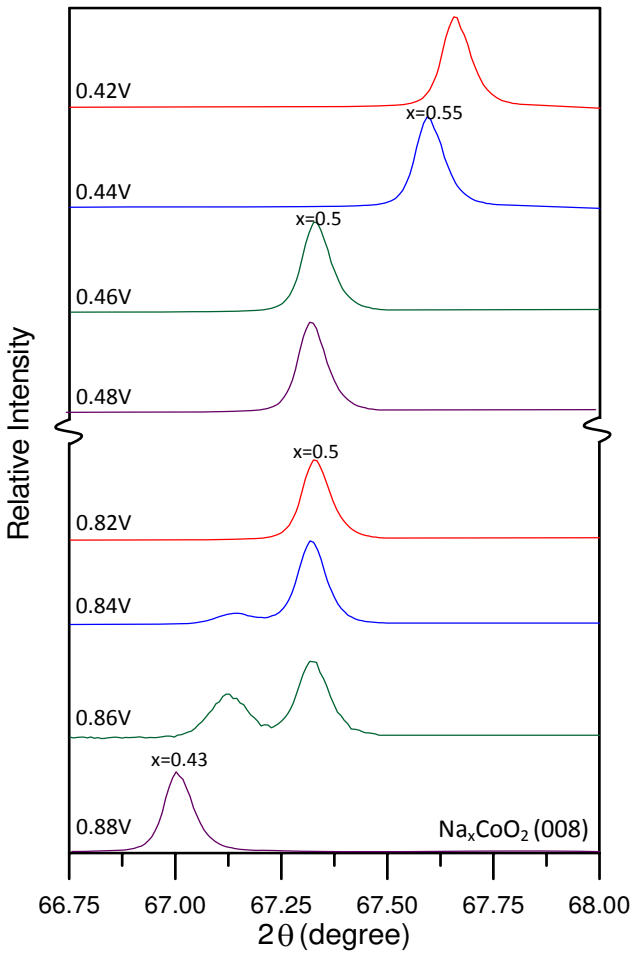

FIG. 5: (Color online) X-ray diffraction scans of the (008) peak for different applied voltages near $x = 0.5$. For $x \geq 0.5$, all of our crystals appear to be single phase. For $x \leq 0.5$, two-phase coexistence is observed for the range between $x = 0.5$ and $x = 0.43$

.

4. *Magnetic properties*

Additional evidence of phase purity is provided by magnetic susceptibility measurements. Figure 6 displays the complete susceptibility data measured under a magnetic field of 1 Tesla applied along the ab-direction. These results are consistent with most of the studies reported so far: magnetic behavior evolves from Curie-Weiss-like to Pauli-like as Na ions are de-intercalated from 0.84 to 0.25, without any trace of CoO or Co_3O_4 impurity.[3,34,36,37] Assuming identical Van Vleck susceptibility contribution for the Pauli paramagnetic metal region, the temperature independent portion of the average susceptibility (χ(300K)) should be proportional directly to the density of states at the Fermi level. The susceptibility at $T = 300$ K χ(300K) for $x \leq 0.6$ are shown in the inset of Fig. 6, where χ(300K) for $x = 0.33$ appears as a local maximum and x = 0.5 sits at the local minimum. This trend agrees well with γ values extracted from specific heat measurement, where γ is directly proportional to

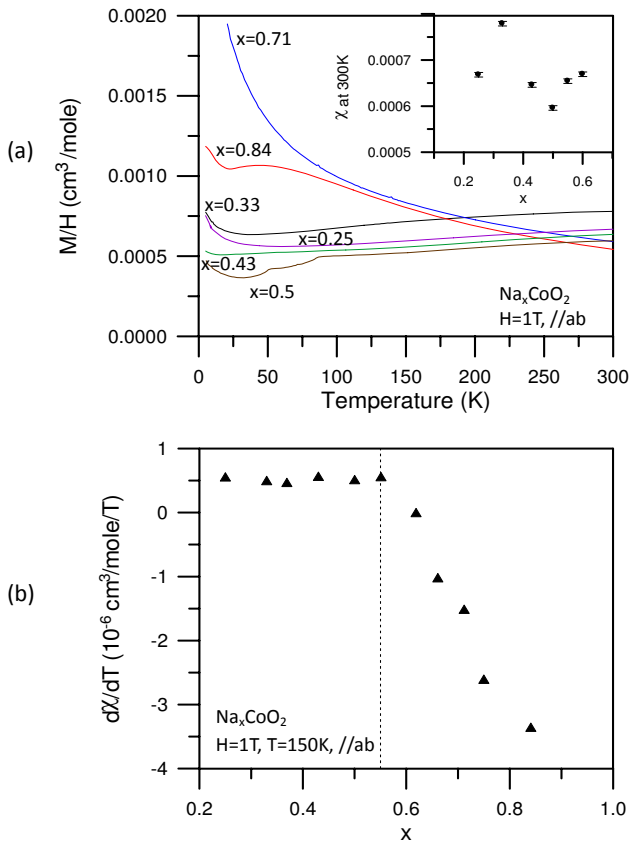

FIG. 6: (Color online) (a) Magnetic susceptibility versus temperature for crystals measured under applied field of 1 Tesla along the *ab*-direction. The value of the susceptibility at $T = 300$ K has been plotted in the inset, which has a maximum near $x = 0.33$ and a minimum near $x = 0.50$. (b) The slope of the average susceptibility versus T at 150 K is plotted against x. There appears to be a crossover near $x = 0.55$.

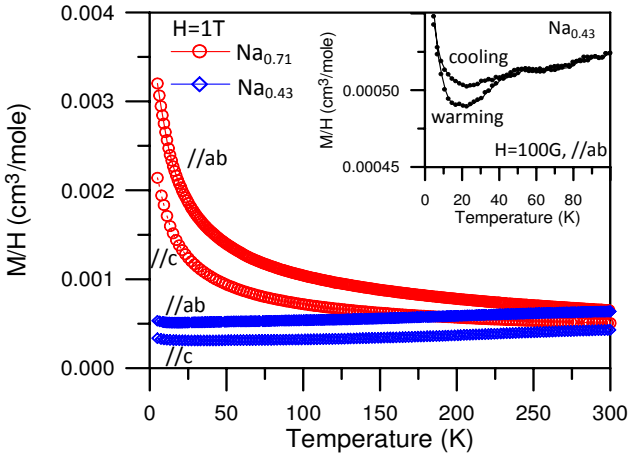

FIG. 7: (Color online) Magnetic susceptibility versus temperature for $Na_{0.71}CoO_2$ and $Na_{0.43}CoO_2$, with $H = 1$ Tesla for both $H//c$ and $H//ab$ directions. The inset shows a low field measurement for $Na_{0.43}CoO_2$ using 100 Oe under zero-field-cooled and field-cooled conditions.

the density of states at Fermi level.[38] The enhancement of density of state at Fermi level for $x = 0.33$ reflects its unique superconducting properties after hydration.[1] The local minimum of χ(300K) for $x = 0.5$ also indicates its proximity to the insulating state that sets in below $T = 51$ K.[3] The slope of the spin susceptibility at 150K in Fig. 6a is an indicator that separates Curie-Weiss (negative) and Pauli (positive) behaviors.[37] The crossover point is close to $x = 0.55$ as shown in Fig. 6b, which is consistent with the crossover points that have been observed in Fig. 1 of Na self diffusion and *c*-lattice parameter as shown in Fig. 4. In Fig. 6a, the in-place susceptibility χ_{ab}(T) for $x = 0.71$ and $x = 0.84$ are nearly identical above $\sim$ 100K, but x = 0.71 does not show any magnetic ordering down to 1.8 K. This behavior suggests $x = 0.71$ is the first equilibrated phase below $x = 0.85$ that does not possess the well known A-type AF ordering below 22-28 K.[2,29] Magnetic properties of the newly identified $Na_{0.71}CoO_2$ and $Na_{0.43}CoO_2$ compositions are summarized in Fig. 7. The Curie-Weiss-like low temperature upturn for $x = 0.71$ agrees very well with the recent ^{23}Na NMR Knight shift data on samples with $x \sim 0.7$.[39]

Powder average of χ_{ab} and χ_c can be fitted to a simple relationship of $\chi(T) = \chi_\circ + C/(T - \Theta)$.[36] Fitting over the temperature range $T = 50 - 250$ K yields $C = 0.078$ cm^{3}K/mole and $\Theta \sim$ -42K. In a simple ionic picture, this corresponds to about a 72% concentration of Co^{4+} ions that participate in the weak antiferromagnetically correlated paramagnetic behavior. Then the electrons on the remaining $\sim$28% of the Co ions are itinerant. We speculate that a special Na ion ordering of $x = 0.71$ may form a large supercell that provides the underlying potential for such partial charge delocalization.

$Na_{0.43}CoO_2$ shows Pauli-like behavior just like all other samples with $x \leq 0.55$. However, low field measurement revealed a weak thermal hysteretic behavior below $\sim$40 K as shown in the inset of Fig. 7. The hysteresis onset near 40K for $x = 0.43$ is very close to the metal-to-insulator transition found in $x = 0.5$, which seems to suggest the inclusion of nearby $x = 0.5$ phase. In addition, there are traces of weak 51 K and 88 K anomalies observable at the level of a few percent. However, the transition at $\sim$51 K for $x = 0.5$ does not show thermal hysteresis, instead, the onset of hysteresis is found to set in below the weak ferromagnetic phase $\sim$27K.[5] Based on the room temperature structural evidence shown in Fig. 5, we can produce samples with no $x = 0.5$ phase inclusion within the $x = 0.43$ matrix. We cannot rule out the possibility of phase segregation below room temperature. The observed thermal hysteresis of the susceptibility below $\sim$40 K may be related to either weak ferromagnetism or spin glass behavior. For $Na_{0.5}CoO_2$, three phase transitions can be identified at $\sim$27, 51 and 88 K in the magnetic susceptibility measured along the *ab*-direction under low magnetic field, as shown in Fig. 8. The transition at 88 K is due to a novel antiferrmagnetic ordering transition, where the ordered spin arrangement and direction has been deduced from polarized neutron diffraction.[5] The transition at 51 K correlates to a metal-

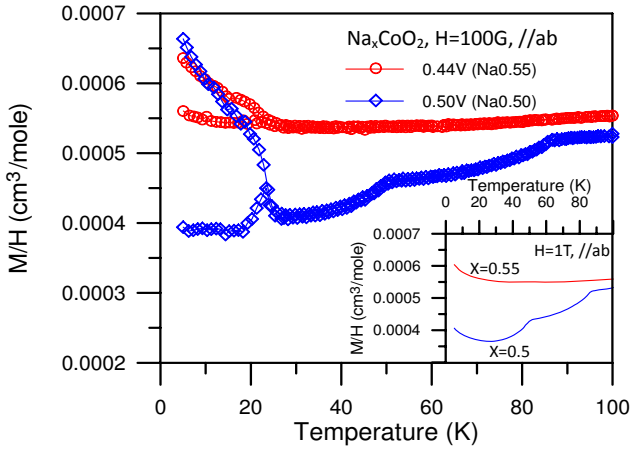

FIG. 8: (Color online) Magnetic susceptibility versus temperature for $Na_{0.55}CoO_2$ and $Na_{0.5}CoO_2$ prepared using 0.44 V and 0.50 V for 24 hours each. The applied field is 100 Oe along the *ab*-direction, and measurements were taken under zero-field-cooled and field-cooled conditions. The inset shows similar measurements with a higher field of 1 Tesla.

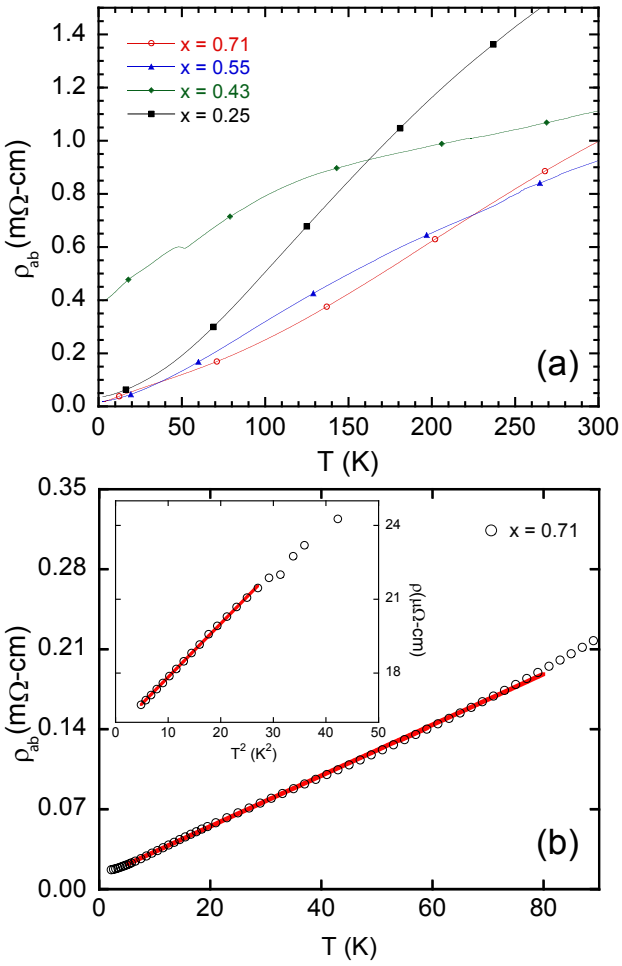

FIG. 9: (Color online) (a) Temperature dependence of the in-plane resistivity for several of the Na_xCoO_2 crystals in the series. (b) Low temperature resistivity of the composition with $x = 0.71$. Two regimes are clearly seen: a T^2 temperature dependence below 5 K (inset) and a T-linear temperature dependence between $\sim$ 5 K and 80 K.

to-insulator transition which may be related to nesting of the Fermi surface.[4] Most of the magnetic measurement results of $Na_{0.5}CoO_2$ at high field before show low temperature upturns below $\sim$30 K of various sizes, usually attributed to trace amount of isolated paramagnetic spins.[40,41] Interestingly, we find the transition at 27 K shows ferromagnetic character with thermal hysteresis at low field as well as field hysteresis at 5 K (not shown). The significant thermal hysteresis found below $\sim$27K for $Na_{0.5}CoO_2$ strongly implies its weak ferromagnetic nature. This transition below 27 K appears to further increase the in-plane resistivity.[5]

The $Na_{0.55}CoO_2$ composition has been previously reported to have a strong in-plane ferromagnetic ordering below $\sim$20K with no magnetic anomalies found near 51 or 88 K.[42] One immediate concern on preparing pure Na_xCoO_2 crystal with $x = 1/2$ is how to separate the potentially mixed phases between $Na_{0.55}CoO_2$ and $Na_{0.5}CoO_2$. A series of fully equilibrated crystals have been prepared with different applied voltage in small steps between 0.40 – 0.50 V; the results of structure evolution are shown in Fig. 5 and magnetic susceptibilities are plotted together with that of $x = 0.5$ in Fig. 8. High field susceptibility measurements show a clear difference: nearly temperature independent behavior for $x = 0.55$ to the one with positive slope for $x = 0.5$. Low field measurements indicates our $Na_{0.55}CoO_2$ crystal has a weak ferromagnetic transition near 27 K without any 51 K or 88 K anomalies, in contrast to $Na_{0.5}CoO_2$. This rules out the possibility of a mixed phase within such a small concentration range. $Na_{0.55}CoO_2$ and $Na_{0.5}CoO_2$ should be considered as two distinctly different phases, although the former is closer to a critical transient state with an extremely narrow dx/dV_{app} plateau as indicated in Fig. 2. We note that the saturated moment and coercive field for $Na_{0.55}CoO_2$ obtained from the electrochemical method is lower than that prepared by the chemical extraction method using iodine/acetonitrile solution.[42] In $Na_{0.5}CoO_2$, the size of the magnetic susceptibility upturn below $\sim$27 K appears to be highly sample dependent in the literature.[4,5,37,41] One major difference between chemical and electrochemical methods has been compared on Li_xCoO_2. Chemical de-intercalation method has a significantly higher charging rate, and thus easier to access the metastable states.[43] We believe the chemical method with a much higher charging rate may yield metastable phases of $Na_{0.55}CoO_2$ of higher weak FM moment, and these may eventually fall into a more equilibrated phase similar to that obtained using the electrochemical route.

5. Transport properties

The transport properties of four of our newly synthesized compositions are summarized in Fig. 9. As shown in Fig. 9(a), the compositions with $x = 0.71, 0.55$, and 0.25 exhibit metallic conductivity, and are consistent with the trend suggested by the phase diagram previously proposed.[3] The sample with $x = 0.43$, does not behave like a good metal and appears to have a large residual resistivity. This particular sample may contain coexisting regions of different phases, such as $x = 0.5$, which are more stable at the local scale. Indeed, after annealing at $T_a = 400$K for several hours (not shown), this sample displays a transition to an insulating regime below $T \approx 50$K, which is a particular feature of the $x = 0.5$ composition[5]. The resistivity of the $x = 0.71$ sample at lower temperatures is shown in detail in Fig. 9(b). A roughly T-linear temperature dependence is observed between ~ 5 K and 80 K, consistent with previous measurements.[3] Fermi liquid behavior is recovered at low temperatures where electron-electron scattering dominates, as noted previously.[44] Here, below ~ 4K the data may be fit by the function of $\rho(T) = \rho_\circ + AT^2$. Our fit (plotted as the solid line) yields values of $\rho = 15.61\ \mu\Omega - cm$ and $A = 0.2226\ \mu\Omega - cm\ K^{-2}$. The residual resistivity $\rho_\circ$ may arise from scattering due to domain boundaries and/or perturbations to the periodic potential felt by electrons within the ab plane, such as defects in the Na arrangement. The observed value of $\rho_\circ$ is about three times smaller than previous measurements[44] and attests to the high homogeneity of the current Na-ordered $x = 0.71$ sample. The value of A, while somewhat smaller than previous measurements, is still relatively large and indicates an large Kadowaki-Woods ratio, $k_{KW} = A/\gamma^2$, assuming γ is similar to previous measurements.[44]

IV. SUMMARY

In summary, we have demonstrated that a non-aqueous electrochemical de-intercalation process can be used to prepare high quality single crystal samples of γ-Na_xCoO_2 with well-defined Na superlattices. The sodium ion self diffusion mechanism has been demonstrated to be well fit by a 1D diffusion model on an aged single crystal. The dominant diffusion species above $x_c \sim 0.53$ is consistent with Na vacancies, and the diffusion coefficient is higher for $x > x_c$, compared to $x < x_c$. The existence of stable phases are reflected in the $dx/dV_{app} = 0$ plateaus, among which $x = 1/2$, $1/3$ and $1/4$ are the most stable. The data suggest that $x \sim 0.75$, 0.55 and 0.43 are somewhat less stable. On the other hand, $x \sim 0.71$ is a very stable phase with a sizeable $dx/dV_{app} = 0$ plateau width. This stable $x = 0.71$ phase is intriguing for its potential Na ordering but without any magnetic ordering down to 1.8K. The absence of A-type AF ordering for $x = 0.71$ and the presence of weak FM in $x = 0.5$ and 0.55 may be related to subtle interactions between the Co ions and the specific potential caused by Na ion ordering, as it is known that Na superstructures can affect the Fermi surface geometry. Clearly more work is required to investigate the effects of Na order across the Na_xCoO_2 phase diagram. Our progress with this electrochemical technique opens the door for further studies of the physical properties of the stable Na ordered phases in single crystal samples.

†corresponding author: fcchou@ntu.edu.tw

Acknowledgments

FCC and GJS acknowledge B. X. Xie's help on fitting of diffusion equation. We acknowledge the helpful discussions with M. W. Chu, Larry Pai, and Patrick Lee. This work was support by the National Science Council of Taiwan under project number NSC-95-2112-M-002. The work at MIT was supported by the U.S. Department of Energy under Grant No. DE-FG02-04ER46134.

[1] K. Takada, H. Sakurai, E. Takayama-Muromachi, F. Izumi, R. A. Dilanian, and T. Sasaki, Nature **422**, 53 (2003).
[2] S. P. Bayrakci, I. Mirebeau, P. Bourges, Y. Sidis, M. Enderle, J. Mesot, D. P. Chen, C. T. Lin, and B. Keimer, Phys. Rev. Lett. **94**, 157205 (2005).
[3] M. L. Foo, Y. Wang, S. Watauchi, H. Zandbergen, T. He, R. J. Cava, and N. P. Ong, Phys. Rev. Lett. **92**, 247001 (2004).
[4] J. Bobroff, G. Lang, H. Alloul, N. Blanchard, and G. Collin, Phys. Rev. Lett. **96**, 107201 (2006).
[5] G. Gasparovic, R. A. Ott, J. H. Cho, F. C. Chou, Y. Chu, J. W. Lynn, and Y. S. Lee, Phys. Rev. Lett. **96**, 046403 (2006).
[6] M. Lee, L. Viciu, L. Li, Y. Wang, M. L. Foo, S. Watauchi, R. A. P. Jr., R. J. Cava, and N. P. Ong, Nature Materials **5**, 537 (2006).
[7] C. Delmas, J. J. Braconnier, C. Fouassier, and P. Hagenmuller, Solid State Ionics **3-4**, 165 (1981).
[8] F. C. Chou, E. T. Abel, J. H. Cho, and Y. S. Lee, J. Phys. Chem. Sol. **66**, 155160 (2005).
[9] L. Balicas, M. Abdel-Jawad, N. E. Hussey, F. C. Chou, and P. A. Lee, Phys. Rev. Lett. **94**, 236402 (2005).
[10] F. C. Chou, J. H. Cho, P. A. Lee, E. T. Abel, K. Matan, and Y. S. Lee, Phys. Rev. Lett. **92**, 157004 (2004).
[11] D. J. Singh, Phys. Rev.B **61**, 13397 (2000).
[12] K. W. Lee, J. Kunes, P. Novak, and W. E. Pickett, Phys. Rev. Lett. **94**, 026403 (2005).
[13] S. Zhou and Z. Wang, Phys. Rev. Lett. **98**, 226402 (2007).
[14] H. B. Yang, S. C. Wang, A. K. P. Sekharan, H. Matsui, S. Souma, T. Sato, T. Takahashi, T. Takeuchi, J. C. Campuzano, R. Jin, et al., Phys. Rev. Lett. **92**, 246403 (2004).

[15] M. Z. Hasan, Y. D. Chuang, D. Qian, Y. Li, Y. Kong, A. Kuprin, A. V. Fedorov, R. Kimmerling, E. Rotenberg, K. Rossnagel, et al., Phys. Rev. Lett. **92**, 246402 (2004).

[16] L. Balicas, J. G. Analytis, Y. J. Jo, K. Storr, H. Zandbergen, Y. Xin, N. E. Hussey, F. C. Chou, and P. A. Lee, Phys. Rev. Lett. **97**, 126401 (2006).

[17] H. W. Zandbergen, M. Foo, Q. Xu, V. Kumar, and R. J. Cava, Phys. Rev.B **70**, 024101 (2004).

[18] P. Zhang, R. B. Capaz, M. L. Cohen, and S. G. Louie, Phys. Rev. B **71**, 153102 (2005).

[19] Y. S. Meng, A. V. der Ven, M. K. Y. Chan, and G. Ceder, Phys. Rev. B **72**, 172103 (2005).

[20] M. Roger, D. J. P. Morris, D. A. Tennant, M. J. Gutmann, J. P. Goff, J.-U. Hoffmann, R. Feyerherm, E. Dudzik, D. Prabhakaran, A. T. Boothroyd, et al., Nature **445**, 631 (2007).

[21] T. Motohashi, E. Naujalis, R. Ueda, K. Isawa, M. Karppinen, and H. Yamauchi, App. Phys. Lett. **79**, 1480 (2001).

[22] H. X. Yang, Y. G. Shi, C. J. Nie, D. Wu, L. X. Yang, C. Dong, H. C. Yu, H. R. Zhang, C. Q. Jin, and J. Q. Li, Mater. Chem. Phys. **94**, 119 (2005).

[23] R. E. Schaak, T. Klimczuk, M. L. Foo, and R. J. Cava, Nature **424**, 527 (2003).

[24] D. Prabhakaran, A. T. Boothroyd, R. Coldea, and N. R. Charnley, Journal of Crystal Growth **271**, 74 (2004).

[25] Y.-J. Shin, M.-H. Park, J.-H. Kwak, H. Namgoong, and O. H. Han, Solid State Ionics **150**, 363 372 (2002).

[26] Y.-I. Jang, B. J. Neudecker, and N. J. Dudney, Electrochemical and Solid-State Letters, **4**, A74 (2001).

[27] K. Takada, K. Fukuda, M. Osada, I. Nakai, F. Izumi, R. A. Dilanian, K. Kato, M. Takata, H. Sakurai, E. Takayama-Muromachid, et al., J. Mater. Chem. **14**, 1448 (2004).

[28] F. C. Chou *et al.*, unpublished

[29] P. Mendels, D. Bono, J. Bobroff, G. Collin, D. Colson, N. Blanchard, H. Alloul, I. Mukhamedshin, F. Bert, A. Amato, et al., Phys. Rev. Lett. **94**, 136403 (2005).

[30] H. Sakurai, S. Takenouchi, N. Tsujii, and E. Takayama-Muromachi, J. Phys. Soc. Jpn. **73**, 2081 (2004).

[31] Q. Huang, B. Khaykovich, F. C. Chou, J. H. Cho, J. W. Lynn, and Y. S. Lee, Phys. Rev. B **70**, 134115 (2004).

[32] W. W. Pai *et al.*, unpublished.

[33] D. P. Chen, H. C. Chen, A. Maljuk, A. Kulakov, H. Zhang, P. Lemmens, and C. T. Lin, Phys. Rev.B **70**, 024506 (2004).

[34] D. Prabhakaran, A. T. Boothroyd, R. Coldea, L. M. Helme, and D. A. Tennant, cond-mat/0312493 (2003).

[35] P. Lemmens, K. Y. Choi, V. Gnezdilov, E. Y. Sherman, D. P. Chen, C. T. Lin, F. C. Chou, and B. Keimer, PRL (2006).

[36] F. C. Chou, J. H. Cho, and Y. S. Lee, Phys. Rev. B **70**, 144526 (2004).

[37] M. Yokoi, T. Moyoshi, Y. Kobayashi, M. Soda, Y. Yasui, M. Sato, and K. Kakurai, J. Phys. Soc. Jpn. **74**, 3046 (2005).

[38] R. Jin, B. C. Sales, S. Li, and D. Mandrus, Phys. Rev.B **72**, 060512 (2005).

[39] I. Mukhamedshin, H. Alloul, G. Collin, and N. Blanchard, cond-mat/0703561 (2007).

[40] H. Watanabe, Y. Mori, M. Yokoi, T. Moyoshi, M. Soda, Y. Yasui, Y. Kobayashi, M. Sato, N. Igawa, and K. Kakurai, 0601538 (2006).

[41] B. Pedrini, J. L. Gavilano, S. Weyeneth, E. Felder, J. Hinderer, M. Weller, H. R. Ott, S. M. Kazakov, and J. Karpinski, Phys. Rev. B **72**, 214407 (2005).

[42] C. H. Wang, X. H. Chen, T. Wu, X. G. Luo, G. Y. Wang, and J. L. Luo, Phys. Rev. Lett. **96**, 216401 (2006).

[43] S. Venkatraman and A. Manthiram, Chem. Mater. **14**, 3907 (2002).

[44] S. Y. Li, L. Taillefer, D. G. Hawthorn, M. A. Tanatar, J. Paglione, M. Sutherland, R. W. Hill, C. H. Wang, and X. H. Chen, Phys. Rev. Lett. **93**, 056401 (2004).